Available online at www.sciencedirect.com

SciVerse ScienceDirect

Geochimica et Cosmochimica Acta 85 (2012) 275–288

Geochimica et Cosmochimica Acta

www.elsevier.com/locate/gca

Sr and $^{87}Sr/^{86}Sr$ in estuaries of western India: Impact of submarine groundwater discharge

Waliur Rahaman *, Sunil Kumar Singh

Geosciences Division, Physical Research Laboratory, Navrangpura, Ahmedabad 380009, India

Received 6 July 2011; accepted in revised form 16 February 2012; available online 5 March 2012

Abstract

Dissolved Sr and $^{87}Sr/^{86}Sr$ are measured in the Narmada, Tapi and the Mandovi estuaries linked to the eastern Arabian Sea. The concentration of dissolved Sr and $^{87}Sr/^{86}Sr$ in the river water endmembers show significant differences reflecting the lithologies they drain. The distribution of Sr in all these estuaries shows a near perfect two endmember mixing between river water and seawater suggesting that there is no discernible net addition/removal of Sr from the estuarine waters. In contrast, $^{87}Sr/^{86}Sr$ shows non-conservative behaviour in all these estuaries, its distribution exhibits significant departure from the theoretical mixing lines. A likely mechanism for this difference in the behaviour between dissolved Sr and its $^{87}Sr/^{86}Sr$ is the discharge of submarine groundwater (SGD) which can modify the $^{87}Sr/^{86}Sr$ of the estuarine waters by exchange with sediments without causing measurable changes in Sr concentration. The impact of such an exchange process on the $^{87}Sr/^{86}Sr$ of the estuaries and therefore on the Sr isotope composition of dissolved Sr entering the Arabian Sea differs among the three estuaries and also between seasons in the Narmada. The non-conservative behaviour of $^{87}Sr/^{86}Sr$ provides a handle to estimate the quantum of SGD to these estuaries. The Sr concentration, $^{87}Sr/^{86}Sr$ ratio and salinity of the submarine groundwater and estimate of its fluxes to the Narmada estuary have been made using inverse model calculations. The model derived SGD flow rates are ~5 and 280 cm/day during pre-monsoon and monsoon, respectively. The more radiogenic Sr isotope composition of SGD relative to the seawater suggests that SGD acts as an additional source of ^{87}Sr to the Arabian Sea.

1. INTRODUCTION

Estuary is the major pathway through which dissolved and particulate materials carried by rivers are transferred to the oceans. The biogeochemical interactions between riverine materials and seawater in estuaries play a key role in determining the flux of elements entering the open oceans. This makes the study of the behaviour of various elements in different types of estuaries important to evaluate their marine budgets and the factors controlling their geochemical behaviour in this transition zone. This study investigates the distribution of Sr and $^{87}Sr/^{86}Sr$ in major estuaries of western India to learn about their behaviour and fluxes to the Arabian Sea. Such studies are directly relevant to the budget of Sr and the evolution of $^{87}Sr/^{86}Sr$ in the oceans. Knowledge of the budget of oceanic Sr and $^{87}Sr/^{86}Sr$ i.e. their sources and sinks in the oceans, is essential as Sr isotope composition of paleo seawater archived in marine deposits are being used for stratigraphic correlation, chronology and also to infer about the impact of temporal variability in tectonics and climate on the isotope evolution. In recent years, these studies have added significance in light of the reports of imbalance in Sr isotope budget in the oceans (e.g. Davis et al., 2003; Allegre et al., 2010).

Available studies on Sr and $^{87}Sr/^{86}Sr$ in estuaries indicate both conservative and non-conservative behaviour (Ingram and Sloan, 1992; Ingram and De Paolo, 1993; Andersson et al., 1994; Wang et al., 2001; Xu and Marcantonio, 2004, 2007; Rahaman and Singh, 2009). For example, non-conservative behaviour of Sr has been observed in the Mississippi estuary and the Baltic Sea due to

* Corresponding author. Present Address: National Centre for Antarctic & Ocean Research, Vasco-da-Gama, Goa 402803, India.
E-mail addresses: waliur@ncaro.org (W. Rahaman), sunil@prl.res.in (S.K. Singh).

0016-7037/$ - see front matter © 2012 Elsevier Ltd. All rights reserved.
http://dx.doi.org/10.1016/j.gca.2012.02.025

chemical speciation and biological processes (Andersson et al., 1994; Xu and Marcantonio, 2004). The strong interaction between sediments and water during high energy conditions in the Changjiang estuary releases Sr to water (Wang et al., 2001) resulting in its non-conservative behaviour. Submarine groundwater discharge (SGD) has been suggested as a potential source of dissolved elements including Sr to coastal oceans (Basu et al., 2001; Charette and Sholkovitz, 2006; Paytan et al., 2006; Johannesson et al., 2010; Lin et al., 2010; Moore, 2010; Huang et al., 2011). Basu et al. (2001) have identified SGD as an important supplier of Sr to the global oceans based on their studies of Sr and $^{87}Sr/^{86}Sr$ in the Bengal basin. The higher $^{87}Sr/^{86}Sr$ ratio observed in coastal waters of the southern Okinawa Trough and the Kao-ping Canyon compared to average seawater is attributed to contribution of radiogenic Sr via recirculated seawater interacting with sediments (Lin et al., 2010; Huang et al., 2011). Some of these findings though bring out the role of SGD in influencing the distribution of Sr and $^{87}Sr/^{86}Sr$ in coastal and estuarine waters, better understanding of its impact in contributing to the marine budget of Sr and its isotopes and their applications to investigate marine processes require investigation on more estuaries. This work presented in this manuscript is a step in that direction.

The goal of this study is to investigate the behaviour of Sr and its isotope composition in three tropical estuaries, the Narmada, Tapi and the Mandovi along the west coast of India. The Narmada and the Tapi are two medium river systems of the Indian peninsular region, flowing mainly through the Deccan basalt in their upstream and the Vindhyan sediments downstream. The Mandovi drains lateritic terrains and the Archean Dharwar craton. All these estuaries are linked to the Arabian Sea.

2. STUDY AREA

The Narmada, Tapi and the Mandovi rivers and their estuaries (Fig. 1) are sampled in this study for their Sr concentration and $^{87}Sr/^{86}Sr$ ratio. This study is a part of our investigations on the behaviour of selected trace elements in Indian estuaries (Rahaman and Singh, 2010; Rahaman et al., 2011). The Narmada originates from Amarkantak in the Vindhyan Mountains in Madhya Pradesh (MP) and flows through Deccan basalts, Vindhyan sediments and alluvium before entering the Gulf of Cambay off Bharuch (Fig. 1). The Tapi originates at Multai in Betal district of MP. It drains the Deccan basalts and alluvial deposits before draining into the Gulf of Cambay off Surat (Fig. 1). The average annual rainfall in the Narmada and the Tapi drainage basins are 1250 and 830 mm, respectively, of this ~90% is received during the south-west monsoon (Gupta and Chakrapani, 2007). The annual discharge of the Narmada is $\sim 47 \times 10^9$ m^3, about 2–3 times that of the Tapi $\sim 19 \times 10^9$ m^3 (Alagarsamy and Zhang, 2005). Both these rivers have dams/reservoirs along their courses.

The Mandovi river originates in the Western Ghats of the Indian peninsula and flows east to west over a length of 75 km through the rocky terrains of Goa, before draining into the Arabian Sea (Upadhyay and Gupta, 1995). The average annual rainfall in this basin is 3000 mm, of which about ~90% occurs during the southwest monsoon (June–September). The average water discharge of the Mandovi is 16×10^9 m^3/y (Upadhyay and Gupta, 1995). A large part of the drainage basin of the Mandovi consists of basalts, phyllites, metagreywacke/metabasalts and schists/gneisses. Most of the lithologies in the basin are capped by laterite deposits that contain bauxites (Sastry and Gopinath, 1985).

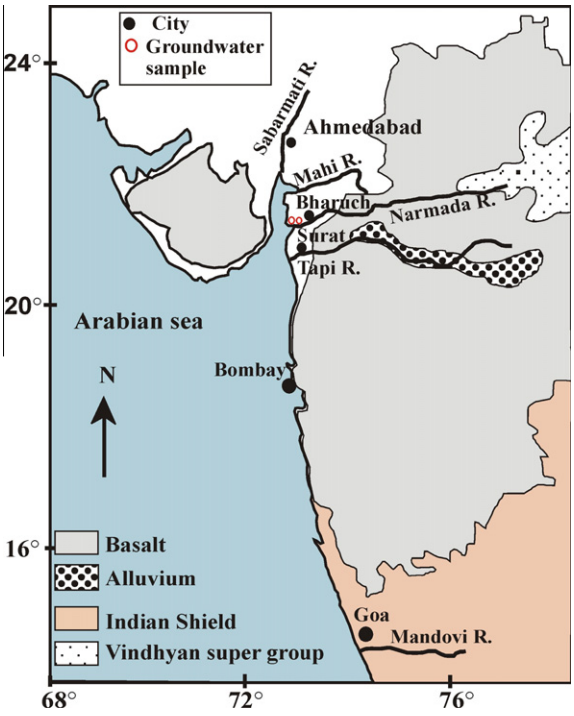

Fig. 1. Location map of the Narmada, Tapi, and the Mandovi river basins. Samples for this study were collected from the estuaries of these rivers.

3. METHODS

3.1. Sampling

Surface water samples were collected from both the rivers and the estuaries during low tide along the salinity gradient. The Narmada estuary was sampled during pre-monsoon (March) and monsoon (July) seasons whereas the Tapi was sampled only during monsoon (July). The Mandovi was sampled during post-monsoon (October). In addition to estuaries, samples were also collected from the rivers upstream, (including samples from up and downstream of the major dams in the Narmada and the Tapi). Two groundwater samples were also collected ~40 km upstream of the Narmada estuary during pre-monsoon (Fig. 1). Salinity, pH and temperature were measured at site. Typically, 2 l of water samples were collected from the surface of the rivers and estuaries. Of this, about 1 l was filtered through 0.2 micron nylon filters in the laboratory within 48 h of sampling. Soon after filtration, an aliquot of the filtered water was acidified to pH ~2 using

double distilled ultra pure HNO_3 and stored for analysis of Sr and other trace elements in precleaned high density polypropylene bottles.

Suspended particulate matter sampling was done only in the Narmada estuary. Towards this, ~10 l of water samples were collected in plastic carbouys and the suspended matter was separated from water by allowing them to settle for 2 days and decanting the supernatant clear water. The slurry containing suspended matter was transferred to suitable containers and brought to the laboratory.

3.2. Measurement of dissolve Sr and $^{87}Sr/^{86}Sr$

Sr concentration and $^{87}Sr/^{86}Sr$ in water samples were determined by isotope dilution in the filtered, acidified samples using thermal ionisation mass spectrometry after chemical separation. The amount of water samples taken for Sr isotope analysis was decided based on their Sr concentration; about 2–10 μg of total Sr is analysed for Sr isotope measurements. Higher amount of total Sr was analysed to get better precision and to minimise the impact of procedural blank. Sr was separated using Eichrom® Sr specific resin (50–100 μm; Horwitz et al., 1992; Pin and Bassin, 1992; Pin et al., 1994; Rai, 2008). The procedure adopted in this study for the extraction of Sr from water samples and the measurement of its isotopic composition is similar to that followed by Rai and Singh (2007). The pure Sr fractions were loaded on degassed high purity Re filaments with dissolved TaO activator. The Sr isotope measurements were carried out using ISOPROBE-T Thermal Ionisation Mass Spectrometer (TIMS) in multi collector static mode. Mass fractionation corrections for Sr were made by normalising $^{86}Sr/^{88}Sr$ to 0.1194. Along with samples, the NBS 987 Sr standard was measured regularly. The average $^{87}Sr/^{86}Sr$ of the NBS 987 Sr standard measured during the period of this study yielded a value of 0.710222 ± 0.000015 (1σ, $n = 13$) well within its recommended value. The Sr concentration and $^{87}Sr/^{86}Sr$ in all the three estuaries are given in Table 1. Several repeat measurements were also made to check the reproducibility, the results of which are listed in Table 2. The precision of measurements of Sr concentration and $^{87}Sr/^{86}Sr$, based on repeat analysis are 0.6% and 0.0008%, respectively (Table 2). The total procedural blank for Sr was ~500 pg, three to four orders of magnitude lower than typical amount of Sr processed in the samples; therefore blank correction was not done.

3.3. Analysis of sediments

Major elements (Na, K, Mg, Ca, Al and Fe) and Sr were measured in suspended sediments collected from the Narmada estuary during pre-monsoon. A known weight (~0.5 g) of sediment samples were ashed at 600 °C and digested by repetitive treatment with HF, HNO_3 and HCl. A few samples were digested in duplicate to check analytical precision. USGS reference standard materials W-1 and G-2 were also analysed following the same analytical procedure to ascertain the accuracy of measurements. Mg, Ca, Al, Fe and Sr were measured using ICP-AES (Jobin Yvon, ULTIMA-2) and Na & K were measured by Flame AAS (Perkin Elmer Model 4000). The analytical precision and accuracy of these measurements is better than 5%.

4. RESULTS

The dissolved Sr and $^{87}Sr/^{86}Sr$ are measured in the estuaries along with salinity, pH and alkalinity. Briefly, in the Narmada estuary, the pH remains within a narrow range of ~8, unlike the Tapi and the Mandovi estuaries which show variation between 7.57–8.02 and 6.61–8.18, respectively (Rahaman and Singh, 2010). Alkalinity lies between 2000 and 3000 μeq/ℓ in the Narmada and the Tapi estuaries where as in the Mandovi it ranges from 384 to 2236 μeq/ℓ (Rahaman et al., 2011). Lower pH and alkalinity in the Mandovi river is due to limited water–rock interaction in its basin, particularly carbonate dissolution. Alkalinity shows an increase in the 4–12 salinity range in the Tapi estuary.

4.1. Dissolved Sr and $^{87}Sr/^{86}Sr$

The concentration of dissolved Sr and its $^{87}Sr/^{86}Sr$ in the three estuaries, the Narmada, Tapi and the Mandovi are presented in Table 1. In addition, the Sr data for the two groundwater samples (depths ~18 and ~24 m) analysed are also given in Table 1. The chemical characteristics of these estuaries are discussed in Rahaman and Singh (2010) and Rahaman et al. (2011).

Dissolved Sr in the Narmada river (salinity $\leqslant 0.2$) displays a range from ~1.4 to 2.1 μmol/kg and from ~1.3 to 1.7 μmol/kg during pre-monsoon and monsoon, respectively (Table 1). Some of the river water samples (NE07-20, 21, 22, NEM07-14; Table 1) were collected near the Sardar Sarovar Dam ~170 km upstream of the estuary. $^{87}Sr/^{86}Sr$ of the river water varies from 0.71001 to 0.71079 and 0.70994 to 0.71053 during these two seasons. The dissolved Sr concentration and its isotope composition in the Narmada river measured in this study (Table 1) is within the range of those reported by Trivedi et al. (1995) and Dessert et al. (2001). Sr isotope composition of the Narmada bears the signatures of Deccan basalts and Vindhyan sediments through which it flows. The two groundwaters display narrow range in Sr isotope composition, 0.70941–0.70951 though their Sr concentrations differ widely, 9.6–57.4 μmol/kg (Table 1). The Tapi estuary was studied only during monsoon. The two river water samples from the Tapi have $^{87}Sr/^{86}Sr$ of 0.70875 and 0.70894, marginally less radiogenic than the Narmada waters. The Sr concentrations in these samples are ~1.3 and ~2.5 μmol/kg, similar to those reported earlier (Trivedi et al., 1995; Dessert et al., 2001). Analogous to the Narmada, the $^{87}Sr/^{86}Sr$ of the Tapi is also dominated by Sr supply from the Deccan basalts which is unradiogenic in Sr (Das et al., 2006). The Mandovi river and estuary were sampled during post-monsoon. The Sr concentration and $^{87}Sr/^{86}Sr$ in the Mandovi river water are ~0.7 μmol/kg and 0.71062, respectively. Among the three rivers, the lowest concentration of dissolved Sr is in the Mandovi, consistent with the lateritic lithology exposed in its drainage basin, its higher runoff and lower water–rock interaction. This inference is also

Table 1
Dissolved Sr concentrations and $^{87}Sr/^{86}Sr$ in the Narmada, Tapi and the Mandovi estuaries.

Sample	Latitude	Longitude	Salinity	Sr (μmol/kg)	S.E. σ_μ (%)	$^{87}Sr/^{86}Sr$	S.E. σ_μ (%)
Narmada (pre-monsoon, March 2007)							
NE07-20	21°49.49′	73°11.57′	0	1.71	0.03	0.71064	0.0013
NE07-21	21°50·02′	73°45.34′	0	1.37	0.02	0.71079	0.0011
NE07-22	21°51.81′	73°41.75′	0	1.41	0.02	0.71076	0.0009
NE07-18	21°40.51′	72°57.00′	0.2	1.94	0.03	0.71006	0.0011
NE07-19	21°40.63′	72°57.54′	0.2	2.05	0.03	0.71001	0.0012
NE07-1	21°40.81′	72°54.57′	4.8	12.37	0.02	0.70939	0.0009
NE07-2	21°41.26′	72°52.60′	9.3	27.35	0.03	0.70929	0.0008
NE07-3	21°40.58′	72°50.39′	11.8	31.12	0.03	0.70933	0.0009
NE07-4	21°39.20′	72°47.42′	15.9	41.53	0.03	0.70922	0.0007
NE07-5	21°38.80′	72°45.34′	18.2	46.29	0.03	0.70919	0.0010
NE07-6	21°40.75′	72°42.05′	20.0	51.29	0.03	0.70921	0.0008
NE07-7	21°40.71′	72°49.83′	21.3	53.82	0.04	0.70918	0.0009
NE07-8	21°39.46′	72°35.89′	22.1	55.86	0.03	0.70921	0.0010
NE07-9	21°39.36′	72°34.51′	23.9	59.78	0.03	0.70919	0.0007
NE07-10	21°39.62′	72°33.28′	25.3	65.11	0.03	0.70915	0.0009
NE07-11	21°38.73′	72°33.02′	25.5	65.19	0.02	0.70919	0.0009
NE07-12	21°38.04′	72°32.70′	27.2	68.03	0.03	0.70917	0.0010
NE07-13	21°38.0′	72°32.7′	29.0	72.72	0.02	0.70920	0.0009
NE07-15	21°37.94′	72°32.05′	31.1	77.08	0.03	0.70915	0.0008
Groundwater upstream Narmada estuary							
GW08-4	22°02.02′	72°50.31′	0.6	9.59	0.05	0.70951	0.0025
GW08-6	22°03.01′	72°47.81′	1.9	57.4	0.13	0.70941	0.0020
Narmada (monsoon, July 2007)							
NEM07-14	–	–	0	1.30	0.02	0.70994	0.0010
NEM07-1	21°40.59′	72°55.58′	0	1.55	0.02	0.71053	0.0009
NEM07-2	21°39.08′	72°46.64′	0.1	1.74	0.02	0.71026	0.0010
NEM07-3	21°40.07′	72°37.12′	1.3	4.38	0.02	0.70942	0.0011
NEM07-4	21°39.58′	72°36.34′	2.2	8.15	0.02	0.70937	0.0011
NEM07-6	21°39.15′	72°34.28′	5.1	13.45	0.02	0.70927	0.0009
NEM07-7	21°38.55′	72°33.18′	6.0	15.16	0.03	0.70926	0.0010
NEM07-8	21°38.39′	72°33.26′	8.0	18.63	0.02	0.70921	0.0010
NEM07-9	21°39.27′	72°35.26′	9.8	24.44	0.04	0.70921	0.0009
NEM07-10	21°38.52′	72°33.2′	12.1	37.40	0.04	0.70918	0.0007
NEM07-11	21°38.81′	72°33.94′	14.1	34.24	0.03	0.70917	0.0010
NEM07-12	21°38.05′	72°33.19′	15.5	37.91	0.02	0.70918	0.0010
NEM07-13	21°38.55′	72°32.93′	17.2	42.40	0.02	0.70918	0.0011
Tapi (monsoon, July 2007)							
TPM07-14	–	–	0	1.32	0.02	0.70875	0.0009
TPM07-1	21°10.56′	72°46.74′	0–0.2	2.48	0.02	0.70894	0.0009
TPM07-2	21°8.9′	72°45.8′	1.1	4.99	0.02	0.70903	0.0009
TPM07-3	21°8.52′	72°43.61′	2.1	7.27	0.02	0.70906	0.0011
TPM07-4	21°8.86′	72°42.26′	3.9	11.17	0.03	0.70909	0.0010
TPM07-5	21°9.15′	72°4.73′	4.9	14.25	0.03	0.70911	0.0009
TPM07-6	21°9.3′	72°40.19′	5.8	16.33	0.02	0.70911	0.0008
TPM07-7	21°7.97′	72°39.58′	7.8	21.22	0.02	0.70910	0.0009
TPM07-8	21°7.05′	72°39.74′	9.8	25.60	0.02	0.70913	0.0008
TPM07-9	21°5.79′	72°39.98′	11.5	29.93	0.03	0.70912	0.0009
TPM07-10	21°4.97′	72°40.64′	13.1	33.41	0.02	0.70915	0.0008
TPM07-11	21°4.41′	72°40.71′	14.9	38.40	0.02	0.70915	0.0008
TPM07-12	21°3·6′	72°40.68′	17.4	44.64	0.02	0.70915	0.0008
TPM07-13	21°3.16′	72°40.35′	20.3	51.22	0.02	0.70915	0.0008
Mandovi (post-monsoon, October 2007)							
MD07-1	15°32.56′	73°57.69′	0–0.1	0.69	0.03	0.71062	0.0007
MD07-2	15°32.39′	73°55.95′	2.7	6.87	0.02	0.70928	0.0009
MD07-3	15°31.55′	73°55.60′	6	14.30	0.03	0.70924	0.0009
MD07-4	15°31.33′	73°55.38′	13.5	32.85	0.05	0.70916	0.0009
MD07-5	15°30.33′	73°54.82′	16.1	39.82	0.04	0.70916	0.0008
MD07-6	15°30.27′	73°54.16′	19.7	48.09	0.03	0.70917	0.0008
MD07-7	15°30.11′	73°52.88′	26.9	65.67	0.02	0.70914	0.0007

(*continued on next page*)

Table 1 (*continued*)

Sample	Latitude	Longitude	Salinity	Sr (μmol/kg)	S.E. σ_μ (%)	$^{87}Sr/^{86}Sr$	S.E. σ_μ (%)
MD07-8	15°30.34′	73°50.63′	31.3	77.75	0.02	0.70917	0.0009
MD07-9	15°29.29′	73°48.40′	33.7	81.90	0.02	0.70915	0.0009
MD07-10	15°29.07′	73°41.09′	33.6	82.78	0.02	0.70912	0.0009

S.E. σ_μ Standard error on the measurements (internal precision).

Table 2
Precision of dissolved Sr and $^{87}Sr/^{86}Sr$ measurements in estuary samples.

Sample	[Sr] (μmol/kg)	Δ_{Sr} (%)	$^{87}Sr/^{86}Sr$	$\Delta_{^{87}Sr/^{86}Sr}$ (ppm)
NE07-1	12.3		0.70939	
NE07-1R	12.2	0.8	0.70940	14.1
NEM07-10	37.4		0.70918	
NEM07-10R	37.1	0.8	0.70918	2.8
TPM-10	29.9		0.70915	
TPM-10R	33.4	10.5	0.70915	1.4
MD07-8	77.7		0.70917	
MD07-8R(1)	77.3	0.5	0.70916	11.3
MD07-8R(2)	76.9	0.5	0.70916	5.6
MD07-8R(3)	77.3	0.5	0.70916	5.6
Average		0.6 ± 0.1*		7.9 ± 4.1

Δ External precision, based on repeat analysis.
[a] Excluding the TPM-10 pair.

corroborated by its lowest alkalinity and concentrations of dissolved U, Mo and Re among the three rivers analysed (Rahaman et al., 2011).

Dissolved Sr and $^{87}Sr/^{86}Sr$ in the Narmada estuary (excluding river samples collected near the Sardar Sarovar Dam) ranges from 1.4 to 77.1 μmol/kg and 0.71006 to 0.70915, respectively for the salinity range 0.2–31 during pre-monsoon whereas during monsoon, it ranges from 1.6 to 42.4 μmol/kg and from 0.71053 to 0.70918 in the salinity range 0–17 (Table 1). This estuary could not be sampled beyond salinity of 17 during monsoon because of inadequate facilities for sample collection in the highly turbulent conditions. The Tapi estuary has Sr and $^{87}Sr/^{86}Sr$ in range of 2.5–51.2 μmol/kg and 0.70894–0.70915, respectively in the salinity range of 0–20.3 (Table 1). Sr concentration and $^{87}Sr/^{86}Sr$ in the Mandovi estuary vary from 0.7 to 82.8 μmol/kg and 0.71062 to 0.70912, respectively in the salinity range of 0–33.6 (Table 1).

4.2. Sr and major elements in particulate matter of the Narmada estuary

The concentrations of Sr and major elements in particulate matter along the course of the Narmada estuary during pre-monsoon are given in Table 3. The Sr concentrations in samples vary from 178 to 284 μg/g with an average of 239 ± 31 μg/g, within the range of Sr in sediments of rivers draining the Deccan basalts, 79–273 μg/g (Das and Krishnaswami, 2006; Das et al., 2006). The abundance of Al in the particulates is almost uniform from fresh water to seawater along the salinity gradient with an average concentration of (8.6 ± 0.3) wt.%.

Table 3
Sr and major element abundances in particulate matter from the Narmada estuary during pre-monsoon.

Sample id	Salinity	Al[a]	Fe	Ca	Mg	Na	K	Sr
		(%wt)						μg/g
NE-SS-1	4.8	9.1	8.8	2.7	2.5	0.5	1.1	178
NE-SS-2	9.3	8.3	8.3	3.2	2.4	0.5	1.2	207
NE-SS-3	11.8	8.6	8.1	3.1	2.3	0.5	1.2	207
NE-SS-5	18.2	8.9	8.4	3.4	2.5	0.7	1.3	236
NE-SS-6	20.0	8.5	8.3	3.4	2.4	0.8	1.4	243
NE-SS-7	21.3	8.3	8.2	3.5	2.4	0.9	1.3	250
NE-SS-8	22.1	8.5	8.5	3.5	2.4	0.6	1.9	259
NE-SS-9	23.9	8.4	8.2	3.5	2.4	0.6	1.3	276
NE-SS-10	25.3	8.2	8.0	3.8	2.3	1.0	1.3	284
NE-SS-11	25.5	9.0	8.8	3.9	2.6	0.9	1.4	253
Average		8.6	8.4	3.4	2.4	0.7	1.3	239

[a] Al data from Rahaman et al. (2011).

5. DISCUSSION

5.1. Behaviour of dissolved Sr in the estuary

During both the seasons, dissolved Sr vs. salinity plots in the Narmada estuary show conservative mixing with correlation coefficient, $R^2 \geqslant 0.99$ (Fig. 2a and b). The data of all samples (except NEM07-10) during monsoon fall on the

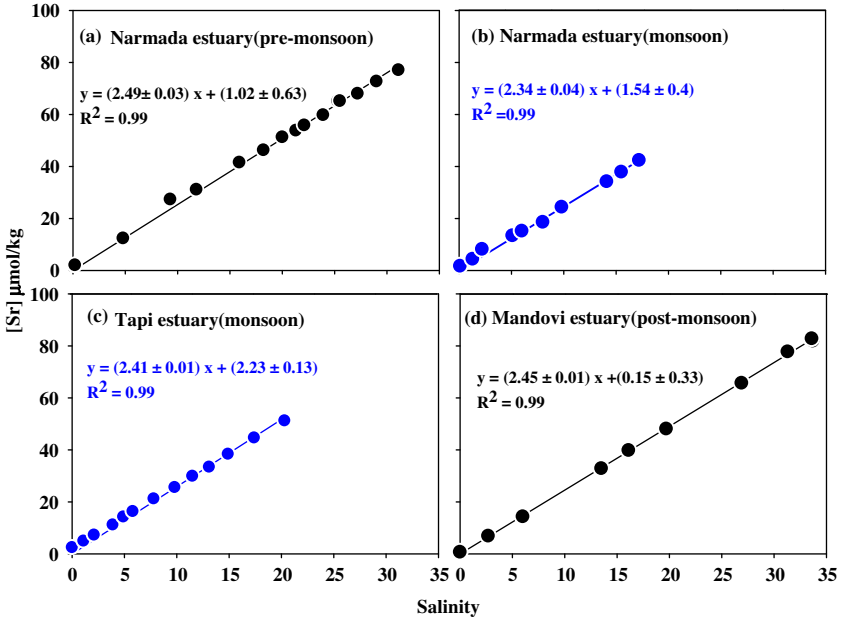

Fig. 2. (a–d) Dissolved Sr vs. salinity plots for the Narmada, Tapi and the Mandovi estuaries. Sr exhibits conservative behaviour in all these three estuaries.

mixing line. The sample NEM07-10 collected during monsoon at salinity 12.1 has Sr concentration of 37.4 µmol/kg (Table 1) which deviates from the trend set by other samples. This sample also shows anomalous behaviour for all the other elements analysed, Re, Mo and U (Rahaman et al., 2011); the reason for which is unclear. This sample, therefore, has not been included in the mixing plot. The intercepts of the mixing lines on the Sr-axis are 1.02 ± 0.63 and 1.54 ± 0.40 (Fig. 2a and b) which overlap with the measured Sr concentration, ~1.5 µmol/kg in the Narmada river. Extrapolation of the mixing lines to 35 salinity yield values of 88.0 ± 1.2 and 83.4 ± 1.5 µmol/kg for Sr concentration of seawater for pre-monsoon and monsoon sampling (Fig. 2a and b); these compare with the value of 88 µmol/kg reported for Sr in the open ocean (Palmer and Edmond, 1989; de Villiers, 1999). The slopes (Sr/salinity) of the mixing lines of the pre-monsoon and monsoon data are nearly the same and quite close to that of seawater. The Sr vs. salinity scatter plots for the Tapi and the Mandovi estuaries also show strong conservative mixing between river water and seawater endmembers with correlation coefficient, $R^2 \sim 0.99$ (Fig. 2c and d). The estimated Sr concentrations at 35 salinity (Fig. 2c and d) are 87.1 ± 0.4 and 85.9 ± 0.5 µmol/kg, respectively consistent with the average seawater concentration deduced from the Narmada data. The distribution of dissolved Sr in the Narmada, Tapi and the Mandovi estuaries (Fig. 2a–d) clearly demonstrate the conservative behaviour of Sr in all of them. The data do not show any measurable loss or gain of Sr in these estuaries during the sampling periods.

The Ca/Al and Sr/Al of the particulate matter in the Narmada estuary increase with salinity (Fig. 3a) most likely a result of increase in biogenic carbonates. Dilution effects by quartz can be ruled out as the Al concentration is nearly uniform through out the salinity range and the plots are normalised to Al. This argument is further confirmed by the property plot Ca/Al–Sr/Al (Fig. 3b) which shows that Sr and Ca increase concomitantly, attributable to incorporation of Sr in calcareous tests.

5.2. Behaviour of dissolved $^{87}Sr/^{86}Sr$ in estuaries

Sr vs. salinity plots (Fig. 2) in all the three estuaries demonstrate conservative mixing of Sr. The observation that almost all the data points fall on the mixing line suggests that, in these estuaries there is no gain or loss of Sr discernible within analytical uncertainty. The average precision of Sr concentration measurements based on replicate analysis of estuarine waters is 0.6%; therefore any gain and loss of Sr within ~1% ($\pm 2\sigma$) is difficult to ascertain conclusively from its distribution in the estuary. In contrast, the precision of $^{87}Sr/^{86}Sr$ determination is better than 0.0008% (8 ppm) (Table 2). This suggests that $^{87}Sr/^{86}Sr$ variations in excess of 0.0020% (20 ppm) can be measured reliably making it a more sensitive tracer to investigate the mixing behaviour of dissolved Sr in estuaries. Thus, small deviations in $^{87}Sr/^{86}Sr$ from theoretical mixing line (TML) (>20 ppm) arising from the supply of Sr from additional source(s) with isotope composition different from river and seawater endmembers can be detected on the $^{87}Sr/^{86}Sr$ vs. 1/Sr mixing plot. This indicates that Sr isotope composition in estuary waters may serve as a better tracer to investigate the behaviour of Sr in this zone.

The Sr isotope mixing plots for the estuaries studied are presented in Fig. 4a–d, along with theoretical mixing lines between river and seawater. As all the estuaries investigated are linked to the Arabian Sea, the $^{87}Sr/^{86}Sr$ of this seawater endmember is taken to be the same as that measured in the

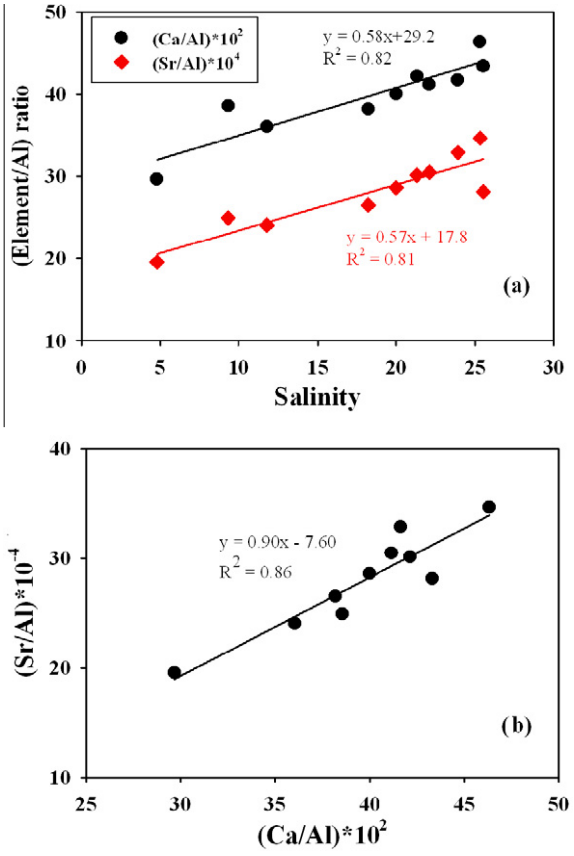

Fig. 3. (a) Scatter plots of Ca/Al and Sr/Al of suspended particulate matter with salinity in the Narmada estuary. Both Ca/Al and Sr/Al show increase with salinity. Ca/Al in (wt.%/wt.%) and Sr (μg/g)/(wt.%). (b) The data in (a) above plotted on Sr/Al vs. Ca/Al diagram. The plot clearly shows the co-variation of Sr and Ca, most likely due to incorporation of Sr in $CaCO_3$ matrix.

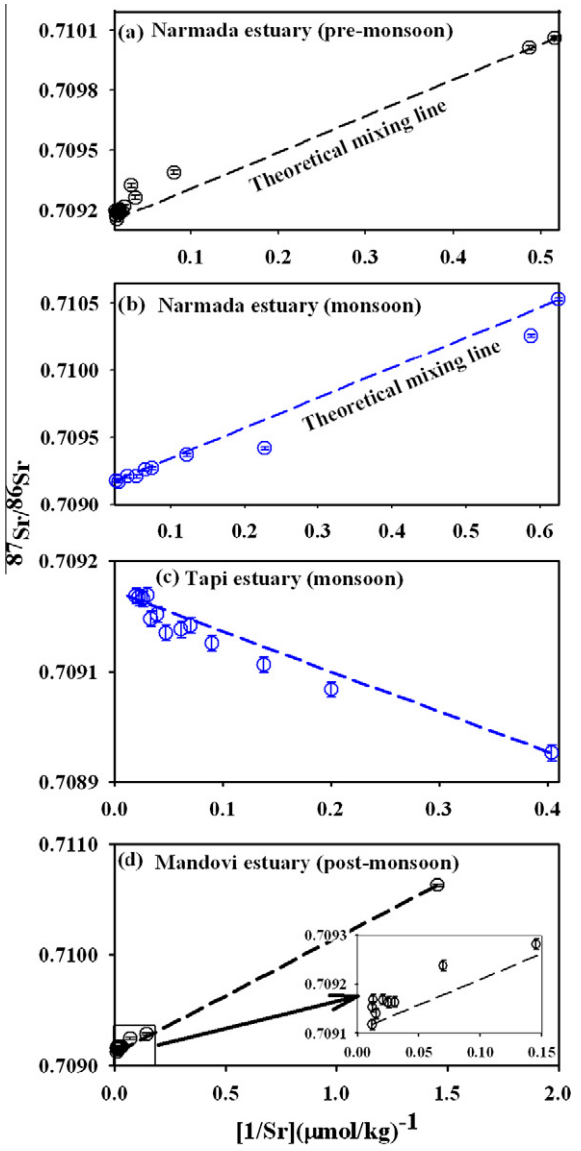

Fig. 4. (a–d) Plots of dissolved $^{87}Sr/^{86}Sr$ vs. 1/Sr concentration. The dashed line is the theoretical mixing line for two end member mixing; river and seawater. Most of the data points plot away from the theoretical mixing line suggesting non-conservative behaviour of $^{87}Sr/^{86}Sr$.

Arabian seawater 0.70915 ± 0.00002 ($n = 5$, Rai, 2008) with Sr concentration of 88 μmol/kg reported for open ocean waters (Palmer and Edmond, 1989; de Villiers, 1999). The Sr mixing diagrams (Fig. 4a–d) show that in all the estuaries, majority of the data points plot away from the theoretical mixing lines between river and seawater. The departure of $^{87}Sr/^{86}Sr$ from TML is in the range of 30–290 ppm, several times the uncertainties associated with repeat measurements of $^{87}Sr/^{86}Sr$ (Table 2). This suggests non-conservative behaviour of $^{87}Sr/^{86}Sr$ through the entire stretch of the estuaries, particularly at higher salinity ranges (Fig. 4). This observation indicates supply of Sr to these estuaries from sources in addition to river and seawater in spite of its near perfect two endmember mixing (Fig. 2). The $^{87}Sr/^{86}Sr$–1/Sr trends (Fig. 4a–d) can result either from desorption/exchange of Sr from particles and/or sediments in the estuaries and/or supply of Sr by SGD such that its impact is discernible only on the distribution of $^{87}Sr/^{86}Sr$ but not on Sr concentration. The SGD may be a mixture of fresh groundwater and re-circulated seawater (Moore, 2010), the mixing proportion being controlled by the hydraulic gradient in adjacent aquifers and tidal conditions in coastal waters (Fig. 5). Some of the earlier studies based on Sr and $^{87}Sr/^{86}Sr$ also reported non-conservative behaviour of Sr in estuaries (Wang et al., 2001; Xu and Marcantonio, 2004, 2007; Lin et al., 2010). These results were attributed to environmental changes (Eh, pH, salinity, temperature) particle–water interactions and other factors such as anoxia and large storms in the coastal areas all of which have the potential to release labile Sr from particulate to dissolve phase. The role of desorption of Sr from particulate phases (Wang et al., 2001) in contributing $^{87}Sr/^{86}Sr$ to the estuaries investigated in the present study remains to be ascertained. Efforts to assess this based on variations in Sr/Al in particles in the estuaries as a function of salinity were unsuccessful because of association of Sr with carbonates. However, the observation that the measured $^{87}Sr/^{86}Sr$ in water

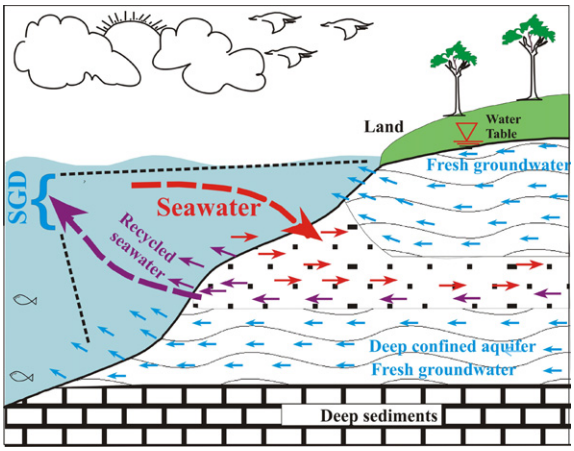

Fig. 5. Schematic of submarine groundwater discharge into coastal regions. Figure modified from Burnett et al. (2006).

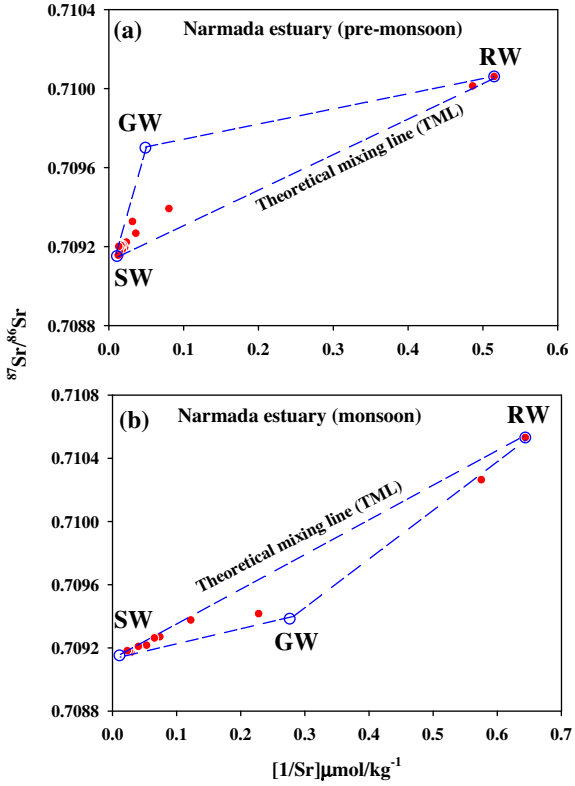

Fig. 6. Plot of $^{87}Sr/^{86}Sr$ vs. 1/Sr in the Narmada estuary. The data points plot above and below the TML during pre-monsoon (a) and monsoon (b), respectively. The deviation of the data points from the TML is explained in terms of three endmember mixing, riverwater, seawater and sub-marine groundwater. The Sr concentration and $^{87}Sr/^{86}Sr$ of the SGD endmembers estimated based on the inverse model is also plotted. SW, RW and GW represent seawater, riverwater and submarine groundwaters.

deviates from TML all along the estuary, particularly at higher salinities (Fig. 4) and this trend is persistent even during pre-monsoon season when particulate transport from rivers is significantly lower seems to indicate that desorption of Sr from particles is unlikely to be an important source of dissolved $^{87}Sr/^{86}Sr$ to these estuaries. This favours SGD as the likely source of additional Sr to the estuaries studied. In this context, it must be mentioned that Krupadam et al. (2006) and Jacob et al. (2009) have reported significant SGD into the Tapi estuary and southwest coast of India, respectively. Further, the important role of SGD in contributing to Sr in estuaries and coastal waters has been brought out in some of the earlier studies. Basu et al. (2001) based on studies of Sr and $^{87}Sr/^{86}Sr$ in groundwaters of the Bengal basin suggested that the Bay of Bengal receives significant input of Sr via SGD, comparable in magnitude to its combined flux from the Ganga–Brahmaputra rivers. Charette and Sholkovitz (2006) based on Sr in subterranean estuary suggested Sr contribution via SGD to seawater even higher than rivers. $^{87}Sr/^{86}Sr$ measurements have been successfully used to evaluate water-mass mixing and the influence of submarine groundwater discharge (SGD) in the Southern Okinawa Trough, South China Sea, and Kao-ping Canyon coastal waters and marginal seas (Huang et al., 2011). The observation in this study that the behaviour of Sr is conservative in the three estuaries whereas $^{87}Sr/^{86}Sr$ is non-conservative, places stringent constraints on the (Sr/salinity) ratio of the SGD supplying Sr to these estuaries, it has to be within uncertainties of that expected from the Sr-salinity mixing line (Fig. 2a–d), but with $^{87}Sr/^{86}Sr$ different from the TML.

In the subsequent section, attempts have been made to characterise the SGD endmember for its Sr concentration and $^{87}Sr/^{86}Sr$ ratios and to estimate the SGD flux based on the Sr isotope budget. These estimates rely on the hypothesis that deviations in $^{87}Sr/^{86}Sr$ from the TML (Figs. 4a and b; 6a and b) is only due to Sr contributions from SGD. The distribution of data on the $^{87}Sr/^{86}Sr$–1/Sr plot during monsoon and pre-monsoon shows that the impact of SGD on the $^{87}Sr/^{86}Sr$ distribution in the Narmada estuary occurs at different salinities (Fig. 6a and b) during these two periods. This can be attributed to differences in the morphology of the river mouth, hydraulic gradient of the coastal aquifer and relationship between water table and local topography. The water discharge of the Narmada during monsoon is orders of magnitude higher than that during pre-monsoon. As a result, the isohaline contours are farther into the sea during monsoon compared to pre-monsoon. For example, the location of the sample NEM07-4 with salinity 2.2 collected during monsoon coincides with that of the sample NE07-8 of salinity ~22.1 during pre-monsoon (Table 1). The maximum deviation of $^{87}Sr/^{86}Sr$ from the theoretical line is observed at locations 21°40′N and 72°37′–72°50′E (Table 6, Fig. 4), therefore, the maximum SGD contribution to the Narmada estuary is also expected at these locations. The impact of SGD on $^{87}Sr/^{86}Sr$ of the estuary during monsoon is opposite to that during the pre-monsoon (Figs. 4a and b; 6a and b). This could be due to lower $^{87}Sr/^{86}Sr$ or Sr concentration or both of SGD to this estuary during monsoon displaying their seasonal variations.

The $^{87}Sr/^{86}Sr$–1/Sr plot of the Tapi estuary shows negative slope with majority of the data plotting below the TML (Fig. 4c). This can arise if $^{87}Sr/^{86}Sr$ of the SGD is lower than that of seawater. Considering that the Tapi drains

Deccan Trap basalts which are generally characterised by unradiogenic Sr, it seems likely that this requirement may be met. In the absence of Sr concentration and $^{87}Sr/^{86}Sr$ data for groundwaters in and around the Tapi basin, quantification of the contribution from SGD to the estuary is difficult. In this context it is pertinent to mention that Krupadam et al. (2006) have reported groundwater flux of 18×10^9 m^3/y to the Tapi estuary.

The river endmember of the Mandovi estuary has lower Sr concentration with more radiogenic Sr than those of the Narmada and the Tapi. However, similar to the Narmada and the Tapi estuaries, two endmember $^{87}Sr/^{86}Sr$–1/Sr mixing plot for the Mandovi estuary also shows non-conservative behaviour. In this estuary, many of the samples from the higher salinity region plot above the TML (Fig. 4d). The lithology of the drainage basin of the Mandovi river is more radiogenic in Sr as evident from the riverine $^{87}Sr/^{86}Sr$. Therefore, groundwaters draining this region are also expected to have more radiogenic Sr than that of seawater. If such groundwaters form part of SGD discharging into the estuarine region, it would increase the $^{87}Sr/^{86}Sr$ of the estuary water compared to that defined by the TML (Fig. 4d).

5.3. Characterising SGD and estimate of SGD fluxes in estuaries using inverse modelling

In this study, an inverse model has been used to characterise the SGD (combined freshwater and recycled seawater) based on the distribution of Sr and $^{87}Sr/^{86}Sr$ in the estuary along with knowledge of seawater and riverwater endmember composition. The inverse model has been used successfully to apportion the contribution of cations from different sources to river waters based on *a priori* values for various endmembers (e.g. Negrel et al., 1993; Gaillardet et al., 1999; Tripathy and Singh, 2010). In this study the calculations have been made only for the Narmada estuary (Fig. 6a and b) as the deviations in $^{87}Sr/^{86}Sr$ from TML is less pronounced in the Tapi and the Mandovi estuaries. The *a priori* values of Sr and $^{87}Sr/^{86}Sr$ for the SGD entering the Narmada estuary are assumed to be the same as that measured in one of the two groundwaters. The calculated values of Sr concentration, $^{87}Sr/^{86}Sr$ and salinity of the SGD contributing to the Narmada estuary represents the best fit values consistent with the various measured parameters (i.e. salinity, dissolved Sr and $^{87}Sr/^{86}Sr$) in the estuary.

Details of the modelling approach and calculations are the same as that followed by Tripathy and Singh (2010) for river water source apportionment. The calculation is based on the mass balance equations for salinity, Sr and $^{87}Sr/^{86}Sr$ in the estuary and *a priori* values of these parameters for the three endmembers i.e. seawater, riverwater and SGD (Fig. 6a and b). The relevant equations are

$$\text{Salinity}_m = \sum_{i=1}^{n} \text{Salinity}_i \times f_i \quad (1)$$

$$\text{Sr}_m = \sum_{i=1}^{n} \text{Sr}_i \times f_i \quad (2)$$

$$\left(\frac{^{87}\text{Sr}}{^{86}\text{Sr}}\right)_m \times \text{Sr}_m = \sum_{i=1}^{n} \left(\frac{^{87}\text{Sr}}{^{86}\text{Sr}}\right)_i \times \text{Sr}_i \times f_i \quad (3)$$

$$\sum_{i=1}^{n} f_i = 1 \quad (4)$$

where $i = 1$–3 and represents the three endmembers, i.e. seawater, riverwater and SGD and the subscript m represents the measured values. f_i is the fraction of water contributed to the estuary from source i.

Eqs. (1)–(4) represent budgets of salinity, Sr concentration, $^{87}Sr/^{86}Sr$ and fractional contribution from these sources. The best possible set for model parameters and their associated uncertainties were obtained from Eqs. (1)–(4) using nonlinear weighted fit following the Quasi-Newton method (Tarantola, 2005; Tripathy and Singh, 2010).

Sr concentrations, $^{87}Sr/^{86}Sr$ and salinity of two of the three endmembers, seawater and riverwater are known and are given in Table 4. As discussed in the earlier section, the $^{87}Sr/^{86}Sr$ of the seawater endmember is taken to be the same as that measured in the Arabian seawater 0.70915 ± 0.00002 ($n = 5$, Rai, 2008) with Sr concentration of 88 μmol/kg reported for open ocean waters (Palmer and Edmond, 1989; de Villiers, 1999) at salinity 35 (Table 4). River water endmembers are based on the measured values of samples collected during both monsoon and pre-monsoon periods. For the third endmember, SGD, there is no Sr data, therefore the *a priori* value for this endmember is assumed to be same as that measured in one of the nearby groundwaters (GW08-6). Similarly, for calculating the

Table 4
Salinity, Sr and $^{87}Sr/^{86}Sr$ in seawater, river waters and SGD endmember.

Component	Salinity	[Sr] (μmol/kg)	$^{87}Sr/^{86}Sr$	ε_{Sr}
Pre-monsoon				
Seawater	35	88	0.70915 ± 0.00002[a]	0.0
Riverwater[b]	0.2	1.9	0.71006 ± 0.00001	12.8 ± 0.14
SGD (*a priori*)[c]	1.9 ± 1.0	57.4 ± 20	0.70941 ± 0.00014	3.7 ± 2.0
Monsoon				
Seawater	35	88	0.70915 ± 0.00002[a]	0.00
Riverwater[b]	0	1.6	0.71053 ± 0.00001	19.4 ± 0.14
SGD (*a priori*)[c]	1.9 ± 1.0	57.4 ± 20	0.70941 ± 0.00014	3.7 ± 2.0

[a] Arabian Sea data (Rai, 2008).
[b] Measured in river water during pre-monsoon and monsoon.
[c] Assumed to be the same as in GW08-6 (Table 1).

fractions of water from different endmembers *a priori* values are assumed to be ~50 ± 50%.

The numerical values of $^{87}Sr/^{86}Sr$ ratios are too small compared to the other parameters used in the model (Sr concentration and salinity). Therefore to make the model sensitive to $^{87}Sr/^{86}Sr$, its values have been expressed as ε_{Sr} defined as

$$\varepsilon_{Sr} = \left[\left(\frac{R - R_{sw}}{R_{sw}}\right) \times 10^4\right] \quad (5)$$

The R_{sw} is $^{87}Sr/^{86}Sr$ ratios of seawater and R is $^{87}Sr/^{86}Sr$ ratios measured in estuary water and that of the endmembers.

The model calculation yields *a posteriori* values of Sr concentration, $^{87}Sr/^{86}Sr$ ratio and salinity of the SGD endmember (Table 5) and the fraction of water supplied from the three endmembers to the estuary samples during pre-monsoon and monsoon (Table 6). Sr concentration and $^{87}Sr/^{86}Sr$ of the SGD endmember derived from the inverse model are 20.6, 3.6 μmol/kg and 0.70971, 0.70938 with salinity of 6.4 and 0.7 during pre-monsoon and monsoon, respectively (Table 5, Fig. 6a and b). The model derived parameters show seasonal variations in the SGD endmember with higher values during pre-monsoon (Table 5). The Sr concentration of the SGD calculated for the pre-monsoon and monsoon seasons using the inverse model is close to that expected from their salinity and Sr vs. salinity relations observed in the Narmada estuary (Fig. 2a and b). The deduced salinity of the SGD indicates that it is recycled estuary water. Water from the Narmada estuary enters the local aquifer during high tide and returns to the estuary during low tide (Sinha et al., 2010). In this cycling process

Table 5
A-posteriori values of SGD contributing to the Narmada estuary.

Component	Salinity	[Sr] (μmol/kg)	$^{87}Sr/^{86}Sr$	ε_{Sr}
Pre-monsoon				
SGD	6.4 ± 1.8	20.6 ± 4.3	0.70971 ± 0.00015	7.9 ± 2.0
Monsoon				
SGD	0.7 ± 0.3	3.6 ± 0.7	0.70938 ± 0.00006	3.3 ± 0.8

Table 6
Estimated contribution of seawater, river water and SGD along the salinity gradient in the Narmada estuary.

Sample	Location		Salinity	Contribution of water flux (%)		
	Latitude	Longitude		Seawater	River water	SGD
Pre-monsoon						
NE07-18	21°40.51′	72°57.00′	0.2	0.2	92.7	1.1
NE07-19	21°40.63′	72°57.54′	0.2	0.3	92.5	1.2
NE07-1	21°40.81′	72°54.57′	4.8	9.4	75.4	14.2
NE07-2	21°41.26′	72°52.60′	9.3	24.9	56.3	18.8
NE07-3	21°40.58′	72°50.39′	11.8	25.0	33.5	41.9
NE07-4	21°39.20′	72°47.42′	15.9	41.8	39.2	19.2
NE07-5	21°38.80′	72°45.34′	18.2	49.2	39.4	11.3
NE07-6	21°40.75′	72°42.05′	20.0	52.8	26.6	21.1
NE07-7	21°40.71′	72°49.83′	21.3	58.1	31.3	10.7
NE07-8	21°39.46′	72°35.89′	22.1	57.9	20.3	22.7
NE07-9	21°39.36′	72°34.51′	23.9	61.9	14.3	25.5
NE07-10	21°39.62′	72°33.28′	25.3	74.4	10.4	0.5
NE07-11	21°38.73′	72°33.02′	25.5	68.9	12.6	20.5
NE07-12	21°38.04′	72°32.70′	27.2	74.5	15.9	10.7
NE07-13	21°38.0′	72°32.7′	29.0	75.1	4.2	29.7
NE07-15	21°37.94′	72°32.05′	31.1	87.2	9.7	1.6
Monsoon						
NEM07-1	21°40.59′	72°55.58′	0.01	0.1	98.6	3.5
NEM07-2	21°39.08′	72°46.64′	0.1	0.3	86.8	8.9
NEM07-3	21°40.07′	72°37.12′	1.3	1.9	27.2	67.9
NEM07-4	21°39.58′	72°36.34′	2.2	6.9	78.2	17.8
NEM07-6	21°39.42′	72°35.49′	5.1	13.3	65.3	22.6
NEM07-7	21°39.15′	72°34.28′	6.0	15.6	72.4	14.5
NEM07-8	21°38.39′	72°33.26′	8.0	19.3	40.3	39.8
NEM07-9	21°39.27′	72°35.26′	9.8	26.2	58.8	16.9
NEM07-11	21°38.52′	72°33.2′	14.1	37.1	10.4	50.3
NEM07-12	21°38.81′	72°33.94′	15.5	41.8	35.2	23.7
NEM07-13	21°38.05′	72°33.19′	17.2	46.9	56.9	5.6

the estuary water exchanges its Sr pool with that in the sediments/aquifer solids in such a way that it makes the $^{87}Sr/^{86}Sr$ of the SGD more radiogenic without measurable changes in its Sr concentration. Similar effect of exchange has been reported on the Sr isotope composition of interstitial waters of marine sediments (Elderfield and Gieskes, 1982). Sediments of the Narmada river are more radiogenic in Sr compared to seawater/ estuary water of the Narmada. Therefore, exchange of Sr isotopes between these sediments and estuary water will make the $^{87}Sr/^{86}Sr$ of the SGD more radiogenic. Further, it has been suggested that radiogenic ^{87}Sr produced by the decay of ^{87}Rb may be preferentially released during weathering (Blum and Erel, 1997; Colin et al., 1999) from aquifer sediments to SGD. Such a process can also alter the $^{87}Sr/^{86}Sr$ of the SGD without modifying its Sr concentration. The impact of SGD in the Narmada estuary is observed upstream of 21°40′N and 72°36′E with salinities lower than 22.1 and 2.2 during pre-monsoon and monsoon.

The SGD contribution to the water budget of the Narmada estuary at various salinities shows a wide range; from ~1–42% and 3–68% (Table 6; Fig. 7), respectively during pre-monsoon and monsoon. In general, SGD contributes about 20% of water to the estuary (Fig. 7). The uncertainties associated with the best fit estimates of model parameters are given in Table 5. These range from 1% to 9% for the three components during the two seasons. The uncertainties on seawater fraction decrease with increasing salinity and vice versa in the case of river and SGD endmembers.

The contribution of SGD to the water flux of the Narmada estuary is calculated using the relation:

$$Q_{SG} = f_{\max} Q_{riv} \quad (6)$$

where f_{max} is the maximum SGD to river water ratio measured in the estuary (e.g. NE07-3 in the Narmada pre-monsoon) and Q the discharge, the subscripts SG and riv representing sub-marine groundwater and river water, respectively. The water flux of the Narmada river is highly variable from monsoon to pre-monsoon and hence the SGD rates also vary accordingly. The pre-monsoon and monsoon samples were collected during March and July, 2007, respectively. Water discharge of the Narmada during March and July are 73 and 2189 m^3/s (http://www.grdc.sr.unh.edu/html/Polygons/P2853200.html). These yield SGD fluxes of ~100 and ~5500 m^3/s during these two seasons. This corresponds to SGD flow rates of ~5 and ~280 cm/day considering the area of the Narmada estuary impacted by SGD, ~170 km^2. The SGD flow rates in the Narmada are consistent with those reported from the southwest coast of India using dissolved ^{222}Rn (Jacob et al., 2009) and those from other coastal regions of the world which are in the range of 10–100 cm/day (Burnett et al., 2003a,b and references therein). The SGD flow rates in the Narmada estuary display seasonal variation with higher flow during monsoon. Similar seasonal variation with varying time gap between precipitation and SGD discharge also have been reported for other coastal regions (Michael et al., 2005). Increased water table during monsoon not only increases the supply of fresh groundwater to estuary but also increases the recycled seawater component by pushing the salinity transition zone (STZ) towards the sea as head of the STZ increases its height several times higher than the water table during monsoon (Michael et al., 2005).

The results obtained in this study on dissolved Sr concentration and $^{87}Sr/^{86}Sr$ in the estuaries of the west coast of India bring out the importance of SGD fluxes in modifying the Sr isotope composition of coastal waters and their potential to estimate SGD fluxes. The data show that the SGD fluxes can be constrained better as more systematic data on regional hydrological parameters, Sr and $^{87}Sr/^{86}Sr$ in groundwaters of the region during different seasons become available.

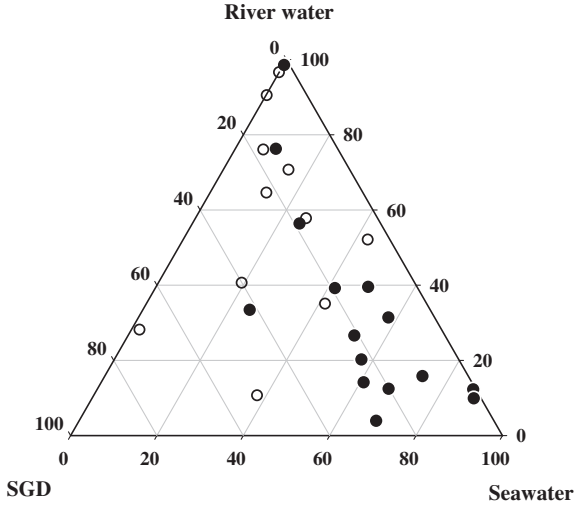

Fig. 7. Ternary diagram of contributions of seawater, riverwater and SGD along the Narmada estuary. The deviation of data points from the mixing line defined by river water and seawater is the measure of contribution from the SGD. Filled and open circles represents pre-monsoon and monsoon samples, respectively.

5.4. SGD flux of Sr from Narmada River to the Arabian Sea

The Sr flux through SGD is calculated to be ~240 × 10^6 mol/year with average $^{87}Sr/^{86}Sr$ ~0.70943 based on the Sr concentration and isotope data in Table 5 and SGD estimated in Section 5.3 during the pre-monsoon and monsoon seasons. For these estimates, the SGD flux for four months during monsoon season is taken to be the same as that of monsoon and for the remaining eight months it is assumed to be same as the flux estimated for pre-monsoon. The Sr flux from the Narmada river is ~76 × 10^6 mol/year based on the water flux of ~47.3 × 10^9 m^3/y with Sr concentration of ~1.5 μmol/kg (Table 1). These estimates though show that the Sr flux via SGD is ~3 times more compared to that of its riverine supply; it does not contribute to the budget of Sr in the Arabian Sea as almost all of it is derived from recycled seawater through coastal sediments and continental aquifers. During this recycling process, the isotope composition of Sr is altered through exchange with aquifer solids and sediments making it more radiogenic, i.e. enriched in ^{87}Sr with respect to the seawater. As a result the SGD serves as an additional source of ^{87}Sr to the Narmada estuary. It can be estimated, based on Sr flux and difference in the

$^{87}Sr/^{86}Sr$ of SGD and seawater, that SGD would supply about 6.2×10^3 mol ^{87}Sr/year to the Arabian Sea through the Narmada estuary. This ^{87}Sr supply from SGD needs to be included in the Sr isotope budget of seawater, however, its impact on both regional and global scale is difficult to asses due to paucity of data from various estuaries and coastal regions.

6. IMPLICATIONS

Evolution of marine Sr isotope during the Phanerozoic has often been used to study the continental/climatic evolution of the earth (Burke et al., 1982; DePaolo and Ingram, 1985; Palmer and Elderfield, 1985; Chaudhuri and Clauer, 1986; Hess et al., 1986; Veizer, 1989; Richter et al., 1992; Blum, 1997; Tripathy et al., 2011). The interpretation of marine Sr isotope records in terms of tectonics/ climate evolution, knowledge of oceanic Sr budget, i.e. its sources and sinks is required. The Sr isotope composition of seawater is determined by contributions of radiogenic Sr through rivers and mantle like unradiogenic Sr delivered by hydrothermal supply and weathering of basalts from volcanic islands (Richter et al., 1992; Davis et al., 2003; Allegre et al., 2010). In these budget estimates of Sr and $^{87}Sr/^{86}Sr$, much attention has not been given to the impact of SGD though its potential role has been indicated in some of the earlier studies (e.g. Basu et al., 2001). The present study has demonstrated that SGD is an additional source of ^{87}Sr to the Arabian Sea. Considering that SGD is a global phenomenon (Burnett et al., 2006), it is very likely that it would serve as a source of Sr isotopes to the world oceans.

The temporal variations in Sr isotope composition of seawater on long time scales has been explained in terms of variations in the relative proportion of supply of radiogenic and mantle like Sr from different sources (Richter et al., 1992; Allegre et al., 2010; Tripathy et al., 2011). In this context, Chaudhuri and Clauer (1986) introduced the concept of 'runout' Sr which represents the Sr supplied to the ocean by subsurface waters to explain the temporal variation in oceanic $^{87}Sr/^{86}Sr$. It was postulated that the runout flux of Sr and its $^{87}Sr/^{86}Sr$ could vary in response to continental break-up/collision and seawater regression/ transgression which in turn could influence seawater Sr isotope composition. The results of the present study contribute to this concept of runout Sr by bringing out its role in contributing to the Sr isotope composition of oceans. Temporal variations in $^{87}Sr/^{86}Sr$ of SGD may be a contributing factor to the marine Sr isotope evolution during the Phanerozoic.

7. CONCLUSIONS

The concentrations of dissolved Sr and its $^{87}Sr/^{86}Sr$ were measured in the Narmada, Tapi and the Mandovi estuaries of western India. The results show that (i) significant differences in Sr and its $^{87}Sr/^{86}Sr$ exist among the river waters which can be understood in terms of the lithologies of the basin they drain, (ii) the plot of Sr vs. salinity in these estuaries show "near perfect" conservative mixing between riverwater and seawater suggesting that there is no measurable net addition or removal of Sr in these estuaries and (iii) the mixing plots of $^{87}Sr/^{86}Sr$ vs. 1/Sr, however, show clearly discernable deviations from the theoretical mixing line, indicating non-conservative behaviour of Sr isotopes in the estuary. The departure of $^{87}Sr/^{86}Sr$ from the theoretical mixing lines is explained in terms of supply of Sr from submarine groundwater discharge with isotopically distinct $^{87}Sr/^{86}Sr$. An inverse model has been used to determine the Sr concentration, $^{87}Sr/^{86}Sr$ ratio and salinity of the SGD endmember contributing to the Narmada estuary. This calculation indicates that SGD in the Narmada estuary is predominantly recycled water which exchanges Sr with the aquifer sediments making it more radiogenic in Sr without changing its Sr concentration. As a result, the SGD acts as source of ^{87}Sr to the Arabian Sea but without discernable supply of Sr. The model calculations also yield data on the fractions of riverwater, seawater and SGD contributing to the estuary at various salinities. The flow rate of SGD in the Narmada estuary is estimated to be 5 and 280 cm/day during pre-monsoon and monsoon, respectively. The SGD in the Narmada estuary supplies 6.2×10^3 moles of ^{87}Sr annually to the Arabian Sea. This study underscores the application of Sr concentration and its isotope composition to quantify the magnitude of submarine groundwater discharge to estuaries and coastal regions.

ACKNOWLEDGEMENTS

Discussions with S. Krishnaswami and his numerous suggestions helped improve the manuscript. The authors thank Gyana Ranjan Tripathy for providing help in inverse modelling calculation and sampling. J.P. Bhavsar, Vineet Goswami, Satinder Pal Singh and Jayati Chatterjee are thanked for their help during sampling. We thank Karen Johannesson for editorial handling and J. Kirk Cochran and two anonymous reviewers for their constructive reviews which improved this manuscript considerably. We thank Ministry of Earth Sciences, Government of India for financial support.

REFERENCES

Alagarsamy R. and Zhang J. (2005) Comparative studies on trace metal geochemistry in Indian and Chinese rivers. *Curr. Sci.* **89**, 299–309.

Allegre C. J., Louvat P., Gaillardet J., Meynadier L., Rad S. and Capmas F. (2010) The fundamental role of island arc weathering in the oceanic Sr isotope budget. *Earth Planet. Sci. Lett.* **292**, 51–56.

Andersson P. S., Wasserburg G. J., Ingri J. and Stordal M. C. (1994) Strontium, dissolved and particulate loads in fresh and brackish waters: the Baltic Sea and Mississippi Delta. *Earth Planet. Sci. Lett.* **124**, 195–210.

Basu A. R., Jacobsen S. B., Poreda R. J., Dowling C. B. and Aggarwal P. K. (2001) Large groundwater strontium flux to the oceans from the Bengal Basin and the marine strontium isotope record. *Science* **293**, 1470–1473.

Blum J. D. (1997) The effect of Late Cenozoic glaciation and tectonic uplift on silicate weathering rates and the marine $^{87}Sr/^{86}Sr$ record. In *Tectonic Uplift and Climate Change* (ed. W. F. Ruddiman). Plenum Press, New York, pp. 259–288.

Blum J. D. and Erel Y. (1997) Rb–Sr isotope systematics of a granitic soil chronosequence: the importance of biotite weathering. *Geochim. Cosmochim. Acta* **61**, 3193–3204.

Burke W. H., Denison R. E., Hetherington E. A., Koepnick R. B., Nelson H. F. and Otto J. B. (1982) Variation of seawater $^{87}Sr/^{86}Sr$ throughout Phanerozoic time. *Geology* **10**, 516–519.

Burnett W. C., Bokuniewicz H., Huettel M., Moore W. S. and Taniguchi M. (2003a) Groundwater and porewater inputs to the coastal zone. *Biogeochemistry* **66**, 3–33.

Burnett W. C., Cable J. E. and Corbett D. R. (2003b) Radon tracing of submarine groundwater discharge in coastal environments. In *Land and Marine Hydrogeology* (eds. M. Taniguchi, K. Wang and T. Gamo). Elsevier Publications, Amsterdam, The Netherlands, pp. 25–43.

Burnett W. C., Aggarwal P. K., Aureli A., Bokuniewicz H., Cable J. E., Charette M. A., Kontar E., Krupa S., Kulkarni K. M., Loveless A., Moore W. S., Oberdorfer J. A., Oliveira J., Ozyurt N., Povinec P., Privitera A. M. G., Rajar R., Ramessur R. T., Scholten J. and Stieglitz T. (2006) Quantifying submarine groundwater discharge in the coastal zone via multiple methods. *Sci. Total Environ.* **367**, 498–543.

Chaudhuri S. and Clauer N. (1986) Fluctuations of isotopic composition of strontium in seawater during the Phanerozoic Eon. *Chem. Geol.* **59**, 293–303.

Charette M. A. and Sholkovitz E. R. (2006) Trace element cycling in a subterranean estuary part 2: Geochemistry of the pore water. *Geochim. Cosmochim. Acta* **70**, 811–826.

Colin C., Turpin L., Bertaux J., Desprairies A. and Kissel C. (1999) Erosional history of the Himalayan and Burman ranges during the last two glacial–interglacial cycles. *Earth Planet. Sci. Lett.* **171**, 647–660.

Das A. and Krishnaswami S. (2006) Barium in Deccan Trap Basalt Rivers: its abundance, relative mobility and flux. *Aquat. Geochem.* **12**, 221–238.

Das A., Krishnaswami S. and Kumar A. (2006) Sr and $^{87}Sr/^{86}Sr$ in rivers draining the Deccan Traps (India): implications to weathering, Sr fluxes, and the Marine $^{87}Sr/^{86}Sr$ record around K/T. *Geochem. Geophys. Geosyst.* **7**, Q06014.

Davis A., Bickle M. J. and Teagle D. (2003) Imbalance in the oceanic strontium budget. *Earth Planet. Sci. Lett.* **112**, 173–187.

DePaolo D. J. and Ingram B. L. (1985) High resolution stratigraphy with strontium isotopes. *Science* **227**, 938–941.

de Villiers S. (1999) Seawater strontium and Sr/Ca variability in the Atlantic and Pacific oceans. *Earth Planet. Sci. Lett.* **171**, 623–634.

Dessert C., Dupre B., Francois L. M., Schott J., Gaillardet J., Chakrapani G. and Bajpai S. (2001) Erosion of Deccan Traps determined by river geochemistry: impact on the global climate and the $^{87}Sr/^{86}Sr$ ratio of sea water. *Earth Planet. Sci. Lett.* **188**, 459–474.

Elderfield H. and Gieskes J. M. (1982) Sr isotopes in interstitial waters of marine sediments from Deep Sea Drilling Project cores. *Nature* **300**, 493–497.

Gaillardet J., Dupre B., Louvat P. and Allegre C. J. (1999) Global silicate weathering and CO_2 consumption rates deduced from the chemistry of large rivers. *Chem. Geol.* **159**, 3–30.

Gupta H. and Chakrapani G. J. (2007) Temporal and spatial variations in water flow and sediment load in the Narmada river. *Curr. Sci.* **92**, 689–684.

Hess J., Bender M. L. and Schilling J. G. (1986) Evolution of the ratio of strontium-87 to strontium-86 from Cretaceous to present. *Science* **231**, 979–984.

Horwitz E. P., Chiarizia R. and Dietz M. L. (1992) A novel strontium-selective extraction chromatographic resin. *Solvent Extr. Ion Exch.* **10**, 313–336, http://www.grdc.sr.unh.edu/index.html.

Huang K., You C., Chung C. and Lin I. (2011) Nonhomogeneous seawater Sr isotopic composition in the coastal oceans: a novel tool for tracing water masses and submarine groundwater discharge. *Geochem. Geophys. Geosyst.* **12**, Q05002.

Ingram B. L. and De Paolo D. J. (1993) A 4300-year strontium isotope record of estuarine paleosalinity in San-Francisco Bay, California. *Earth Planet. Sci. Lett.* **119**, 103–119.

Ingram B. L. and Sloan D. (1992) Strontium isotopic composition of estuarine sediments as paleosalinity–paleoclimate indicator. *Science* **255**, 68–72.

Jacob N., Suresh Babu D. S. and Shivanna K. (2009) Radon as an indicator of submarine groundwater discharge in coastal regions. *Curr. Sci.* **97**, 1313–1320.

Johannesson K. H., Chevis D. A., Burdige D. J., Cable J. E., Martin J. B. and Roy M. (2010) Submarine groundwater discharge is an important net source of light and middle REEs to coastal waters of the Indian River Lagoon, Florida, USA. *Geochim. Cosmochim. Acta* **75**, 825–843.

Krupadam R. J., Smita P. and Wate S. R. (2006) Geochemical fractionation of heavy metals in sediments of the Tapi estuary. *Geochem. J.* **40**, 513–522.

Lin I.-T., Wang C.-H., You C.-F., Lin S., Huang K.-F. and Chen Y.-G. (2010) Deep submarine groundwater discharge indicated by tracers of oxygen, strontium isotopes and barium content in the Pingtung coastal zone, southern Taiwan. *Mar. Chem.* **122**, 51–58.

Michael H. A., Mulligan A. E. and Harvey C. F. (2005) Seasonal oscillations in water exchange between aquifers and the coastal ocean. *Nature* **436**, 1145–1148.

Moore W. S. (2010) The effect of submarine groundwater discharge on the ocean. *Annu. Rev. Mar. Sci.* **2**, 59–88.

Negrel P., Allegre C. J., Dupre B. and Lewin E. (1993) Erosion sources determined by inversion of major and trace element ratios and strontium isotopic ratios in river water: the Congo Basin case. *Earth Planet. Sci. Lett.* **120**, 59–76.

Palmer M. R. and Edmond J. M. (1989) The strontium isotope budget of the modern ocean. *Earth Planet. Sci. Lett.* **92**, 11–26.

Palmer M. R. and Elderfield H. (1985) Sr isotope composition of sea water over the past 75 Myr. *Nature* **314**, 526–528.

Paytan A., Shellenbarger G. G., Street J. H., Gonneea M. E., Davis K., Young M. B. and Moore W. S. (2006) Submarine groundwater discharge: an important source of new inorganic nitrogen to coral reef ecosystems. *Limnol. Oceanogr.* **51**, 343–348.

Pin C. and Bassin C. (1992) Evaluation of a strontium-specific extraction chromatographic method for isotopic analysis in geological materials. *Anal. Chim. Acta* **269**, 249–255.

Pin C., Briot D., Bassin C. and Poitrasson F. (1994) Concomitant separation of strontium and samarium–neodymium for isotopic analysis in silicate samples, based on specific extraction chromatography. *Anal. Chim. Acta* **298**, 209–217.

Rahaman W. and Singh S. K. (2009) Sr in estuaries: impact of submarine ground water discharge. American Geophysical Union, Fall Meeting 2009, abstract OS23A–1182.

Rahaman W. and Singh S. K. (2010) Rhenium in rivers and estuaries of India: sources, transport and behaviour. *Mar. Chem.* **118**, 1–10.

Rahaman W., Singh S. K. and Raghav S. (2011) Dissolved Mo and U in rivers and estuaries of India: implication to geochemistry of redox sensitive elements and their marine budgets. *Chem. Geol.* **278**, 160–172.

Rai S. K. (2008) Isotopic and geochemical studies of ancient and modern sediments. Ph. D. Thesis, MS University Baroda.

Rai S. K. and Singh S. K. (2007) Temporal variation in Sr and $^{87}Sr/^{86}Sr$ of the Brahmaputra: implications for annual fluxes

and tracking flash floods through chemical and isotope composition. *Geochem. Geophys. Geosyst.* **8**, Q08008.

Richter F. M., Rowley D. B. and DePaolo D. J. (1992) Sr isotope evolution of seawater: the role of tectonics. *Earth Planet. Sci. Lett.* **109**, 11–23.

Sastry B. B. K. and Gopinath K. (1985) Bauxite resources of Goa, India. Earth Resources for Goa's Development. Geol. Surv. India, Calcutta, 62–70.

Sinha P. C., Jena G. K., Jain I., Rao A. D. and Husain M. L. (2010) Numerical modelling of tidal circulation and sediment transport in the Gulf of Khambhat and Narmada Estuary, West Coast of India Pertanika. *J. Sci. Technol.* **18**, 293–302.

Tarantola A. (2005) The least square criterion. In *Inverse Problem Theory and Methods for Model Parameter Estimation*. Soc. for Ind. and Appl. Math., Philadelphia, PA, pp. 68–72.

Tripathy G. R. and Singh S. K. (2010) Chemical erosion rates of river basins of the Ganga system in the Himalaya: reanalysis based on inversion of dissolved major ions, Sr, and $^{87}Sr/^{86}Sr$. *Geochem. Geophys. Geosyst.* **11**, Q03013.

Tripathy G. R., Singh S. K. and Krishnaswami S. (2011) Sr and Nd isotopes as tracers of chemical and physical erosion. In *Handbook of Environmental Isotope Geochemistry, Advances in Isotope Geochemistry*, 26 (ed. M. Baskaran). Springer-Verlag, Berlin, Heidelberg, pp. 521–552, http://dx.doi.org/10.1007/978-3-642-10637-8_26.

Trivedi J. R., Pande K., Krishnaswami S. and Sarin M. M. (1995) Sr isotopes in rivers of India and Pakistan: a reconnaissance study. *Curr. Sci.* **69**, 171–178.

Upadhyay S. and Gupta R. S. (1995) The behaviour of aluminium in waters of the Mandovi estuary, west coast of India. *Mar. Chem.* **51**, 261–275.

Veizer J. (1989) Strontium isotopes in seawater through time. *Ann. Rev. Earth Planet. Sci.* **17**, 141–167.

Wang Z., Liu C., Han G. and Xu Z. (2001) Strontium isotopic geochemistry of the Changjiang estuarine waters: implications for water–sediment interaction. *Sci. China Ser. E Eng. Mater. Sci.* **44**, 129–133.

Xu Y. and Marcantonio F. (2004) Speciation of strontium in particulates and sediments from the Mississippi River mixing zone. *Geochim. Cosmochim. Acta* **68**, 2649–2657.

Xu Y. and Marcantonio F. (2007) Strontium isotope variations in the lower Mississippi River and its estuarine mixing zone. *Mar. Chem.* **105**, 118–128.

Associate editor: Karen Johannesson